Feature Article

Polymers and carbon nanotubes—dimensionality, interactions and nanotechnology

Igal Szleifer[a],[**], Rachel Yerushalmi-Rozen[b],[*]

[a]Department of Chemistry, Purdue University, 560 Oval Drive, West Lafayette, IN 47907-2084, USA
[b]Department of Chemical Engineering, The Ilse Katz Center for Meso- and Nanoscale Science and Technology,
Ben-Gurion University of the Negev, 84105 Beer Sheva, Israel

Abstract

The behavior of mixtures of polymers with carbon nanotubes are reviewed. The use of polymers as dispersing agents of individual CNT is described in detail. Two groups of polymer–CNT systems are presented. One corresponds to the case in which the polymer–CNT interactions modify the electronic properties of the tubes. The second case corresponds to the polymers end-tethered to the tubes. This case results in changing the inter-tube interactions from strongly attractive to repulsive, through the entropic (steric) polymer induced repulsions. It is shown that the shape and dimensionality of the tubes determines the strength, range and type of inter-tube van der Waals attractions and polymer induced repulsions. The experimental verification of these ideas, and their implications for tube dispersions and separation are discussed.
© 2005 Elsevier Ltd. Open access under CC BY-NC-ND license.

1. Introduction

Colloids and polymers are intimately related since antiquity. Thousands of years ago in ancient China and the pharos Egypt polymer-stabilized colloidal dispersions were used in inks, paints cosmetics and foods [1]. While trial and error enabled the development of ancient materials technology, fundamental understanding of polymer–colloid interactions and phase behavior has emerged only over the last 30 years or so [2].

An even younger field is that of interactions of polymers with pseudo- one dimensional nano-colloids, known as single walled carbon nanotubes (SWNT) and multi-wall carbon nanotubes (MWNT) [3]. Over the last few years polymers have been utilized for interfacial engineering of SWNT and MWNT in condensed media. Impressive

development of technologies aimed at enabling the incorporation of carbon nanotubes (CNT) into aqueous and organic liquids, solutions, polymer melts, gels, amorphous and crystalline matrices opened new routes for their utilization in a variety of applications.

Following the technological developments, understanding of CNT–polymers interactions is beginning to emerge. It is hoped that knowledge acquired in the fields of colloid science and polymer physics and the tools developed for accounting for complex systems characterized by many degrees of freedom, a large surface-to-volume ratio and synergetic interactions among the different components could be utilized for bridging the current gap between technological development and fundamental understanding.

Here we aim to describe some of the typical behaviors of CNT–polymer systems and discuss their origins. Whereas a comprehensive literature survey of the topic is beyond the scope of this article, we discuss a few examples that highlight the similarities and differences between CNT and classical colloids, while emphasizing the role of reduced dimensionality. Finally, we demonstrate that the physical insight gained from analysis of the different systems may be utilized for devising specific chemical recipes for preparation of CNT–polymer composites.

[**] Tel.: +1 765 494 5255; fax: +1 765 494 5489.
[*] Corresponding authors. Tel.: +972 8 6461272; fax: +972 8 6472916.
E-mail addresses: igal@purdue.edu (I. Szleifer), rachely@bgu.ac.il (R. Yerushalmi-Rozen).

1.1. Individual carbon nanotubes—some essentials

The discovery of CNT [4] (Fig. 1) followed by the development of methods for controlled synthesis of SWNT [5,6] has marked the emergence of the CNT era in materials science and technology, resulting in the publication of more than 20,000 studies since 1991.

SWNT are crystalline graphitic rods, characterized by a diameter in the range of 1–2 nm and a typical length of microns [7] resulting in an aspect ratio (length/diameter) significantly larger than 1000. Individual SWNT exhibit metallic or semiconducting behavior depending on the diameter and spiral conformation (helicity) of the carbon rings (Fig. 2).

These structure–function relations are a consequence of graphite being a 'semi-metal', i.e. a semiconductor with a zero band gap, where structural distortion of the planar graphene sheet can either increase the overlap between the conductance and valence bands, (creating a metallic SWNT) or open a wider band-gap forming a semiconducting SWNT [6,9]. The semi-one-dimensional structure of SWNT leads to ballistic transport in metallic SWNT, enabling them to carry high currents, in the range of 10^9 A/cm^2 [10], with essentially no heating [11]. The electronic properties of MWNT are rather similar to those of SWNT, due to the weak coupling between the cylinders. The combination of their nanometric dimensions, electronic structure and chemical composition [6] results in unique thermal, electrical, mechanical and optical properties. For example, due to the very large aspect ratio and the high rigidity of SWNT [12] they exhibit exceptional strength and
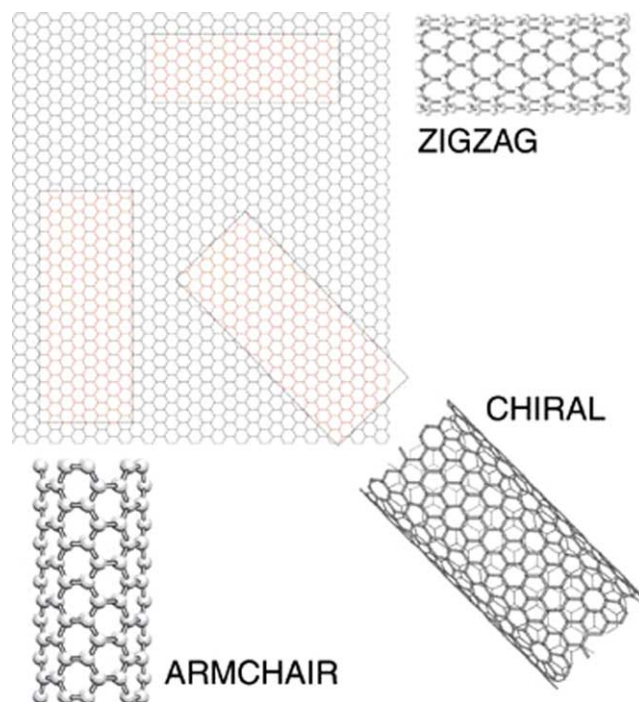
Fig. 2. A schematic image of a graphene layer and SWNT formed by rolling-up of rectangular strips of hexagonal graphite monolayers. The short side of the rectangle becomes the tube diameter and, therefore, is 'quantized' by the requirement that the rolled-up tube must have a continuous lattice structure. Similarly, the rectangle must be properly oriented with respect to the flat hexagonal lattice, which allows only a finite number of roll-up choices, leading to different tube helicities [8].

stiffness as manifested by an elastic Young's modulus of above 1TPa and strength of few tens of GP [13,14].

1.2. Nanotubes for advanced applications

The superb mechanical and electrical properties of carbon nanotubes have raised high expectations regarding their utilization in different fields including molecular electronics and advanced materials: CNT are expected to serve as active components in electronic nano-switches and nano-transistors [15], electron emission sources [16], act as molecular wires connecting components in nano-devices [17], and as chemical sensors [18]. CNT-based nano-composites form a new class of lightweight super strong functional materials for air and space applications [19], energy storage [20] molecular sensors [21] and biomedical applications [22].

The structure and properties described above relate to the individual tube. Yet, these are hard to find: carbon nanotubes emerge from the synthesis as bundles or ropes that contain hundreds of well-aligned SWNT arranged in a close packed triangular lattice (Fig. 3).

The over-micron long ropes further entangle into networks, due to van der Waals (vdW) attraction rendering the carbon-powder insoluble in aqueous and organic liquids, and thus unprocessable. In Fig. 4 we present scanning
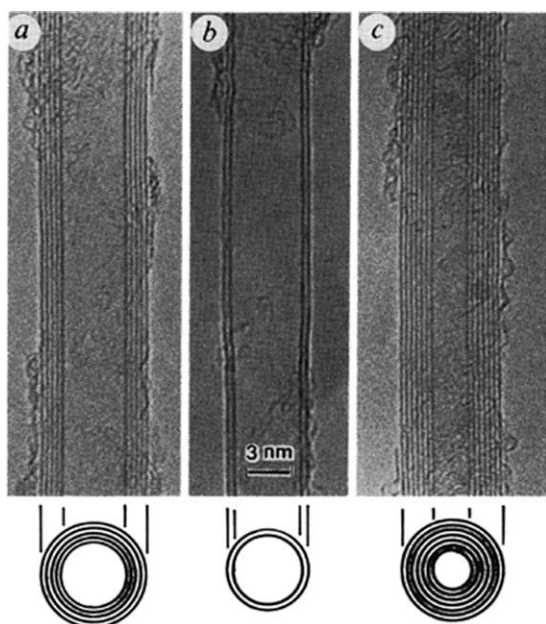
Fig. 1. Electron micrographs of MWNT first discovered by Sumio Iijima in 1991. The Parallel dark lines correspond to the (002) lattice image of graphite. The tubes consist of (a) 5 layers (b) 2 layers (c) 7 layers. Adapted with permission from Ref. [4].
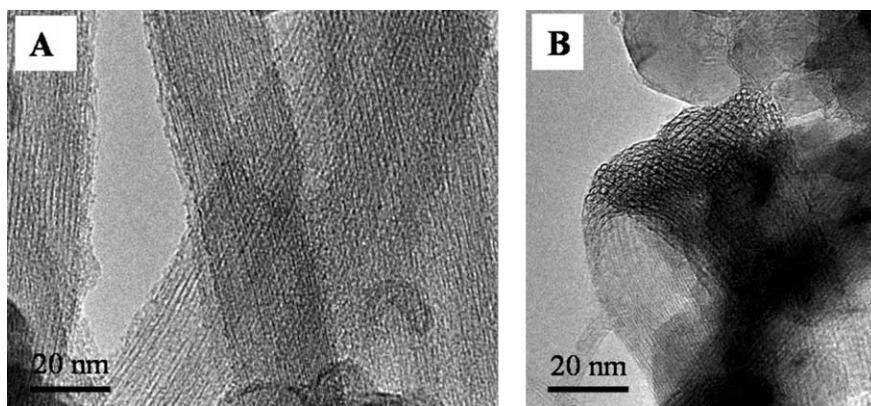
Fig. 3. TEM images of SWNT bundles containing tens of individual tubes (A) typical ropes (B) a bent bundle showing the cross-section of the tubes [23].

electron microscopy micrographs of SWNT powders, synthesized by different methods.

Bundling, aggregation and agglomeration have been identified as the major obstacles for realization of the technological potential of CNT. Whether the final goal is a nanotransistor prepared by placing CNT between two metal electrodes [25] (Fig. 5) a CNT–FET array [26] or a conductive plastic formed by dispersing SWNT (or MWNT) in a polymeric matrix, the ability to exfoliate the bundles into individual tubes and disperse the exfoliated tubes in a liquid medium are necessary prerequisites [27]. For more advanced applications, methods for efficient alignment of nanotubes via the application of external fields (electrical, magnetic or mechanical) and self-assembly into pre-designed three-dimensional structures need to be developed.

Indeed, much effort has been invested over the last years in achieving those goals through different strategies, including chemical functionalization of CNT, covalently linking either monomers, oligomers or polymers, [28], complexation via π–π interactions [29], and adsorption of charged surfactants [30], as demonstrated in Fig. 6.

The approach presented above rely on (sever- to mild) modification of the graphene π-system leading to modification of the electronic structure and the physical properties of the tubes [31]. Recently it was suggested that polymers may offer an alternative, tender, pathway for interfacial engineering of CNT via weak non-specific interactions.
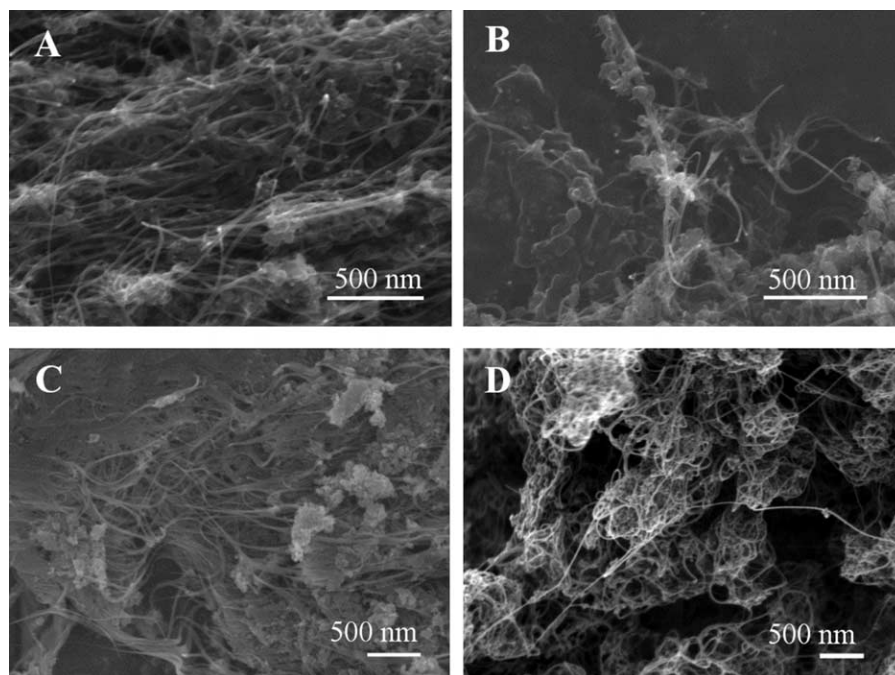

Fig. 4. SEM micrographs of dry powders of SWNT from different sources, showing bundles and ropes of SWNT along with carbonaceous species and the catalyst. The first three (A–C) were synthesized via arc-discharge, while the forth via laser ablation. The individual tubes in the different samples are of similar diameter of 1–1.5, and lengths of hundreds nanometers to about 2 μm [24].
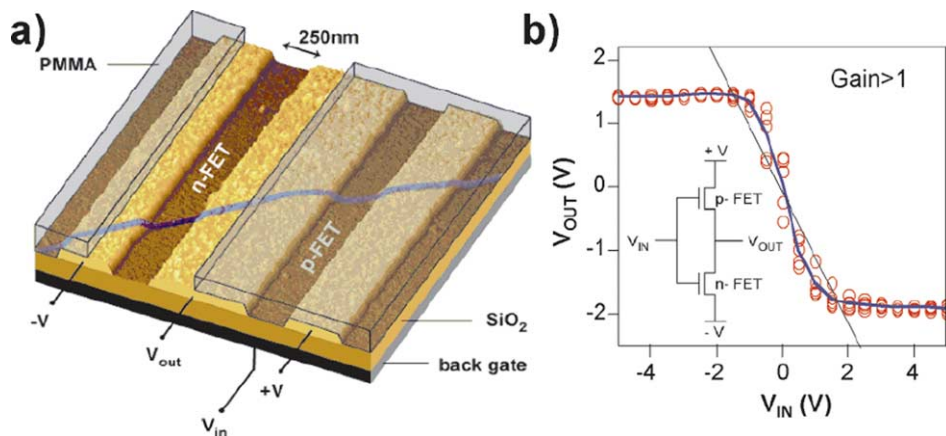
Fig. 5. The IBM group, lead by Ph. Avouri, demonstrated that CNT can be used as the channel in a field effect transistor (FET). In different studies it was found that in a CNT–FET device the electronic characteristics strongly depend on the energy band-gap of the CNT, the contact at the metal–CNT interface, and the thickness of the (gate) oxide layer. In the figure (adapted with permission from Ref. [25]) an AFM image (a) shows a nanotube bundle positioned over gold electrodes to produce two p-type CNTFET in series. The characteristics of the resulting logic gate are presented in (b).

1.3. Polymers enabling nanotechnology

Essentially, polymers can be utilized for achieving each of the goals described above via two very different approaches: being inherently large molecules composed of necklaces of functional groups, polymers may interact with CNT via strong covalent or electrostatic interactions, π-stacking, or hydrogen bonding. These chemical CNT–polymers interactions result in strong coupling between the components, modify the tube surface chemistry and consequentially the intrinsic inter-tube interactions as well as tube-solvent interactions. The range and strength of the resulting interactions depend on the chemical details of the exposed surface, and cannot be easily tuned or generalized.

Alternatively, polymers and CNT may interact via generic weak vdW interactions. Decoration of CNT by adsorbed or end-attached polymer triggers entropic interactions among the polymeric layers. These are long-ranged and do not depend on the detailed chemistry of the CNT–polymer interface. In these cases the range and strength of the interaction can be controlled by the molecular weight and density of the polymeric layers, rather than by the chemical composition of the monomers. Indeed, evidence is emerging that cooperative effect of weak interactions between long-flexible chains and CNT can be utilized for engineering the phase behavior of CNT by modifying the shape, range, and depth of the intermolecular potential, while not affecting the intrinsic properties of the individual tube.

In the following we discuss in detail the two categories and emphasize the synergetic role of tubes geometry, dimensionality and the polymeric length scales.

1.4. Strongly coupled polymer–CNT systems

Strong coupling has been reported in conducting polymers–CNT systems. Conducting polymers are quasi-infinite conjugated π-system, extending over a large
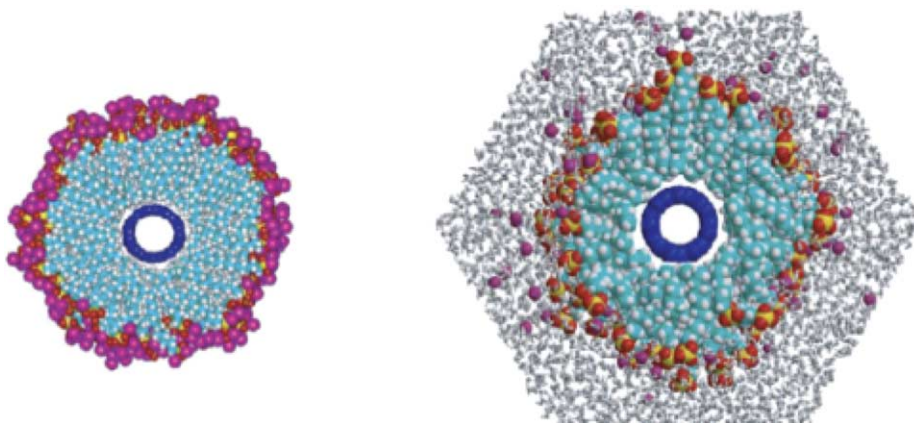

Fig. 6. A simulation showing SWNT embedded within sodium dodecyl sulfate (SDS) micelles (a) individual SWNT embedded in a cylindrical SDS micelle (b) a larger region showing the outer water layer as well. Image (b) indicates that water molecules are excluded from the vicinity of the hydrophobic SWNT. Adapted with permission from Ref. [30] (b).

number of recurring monomer units, resulting in a band-like electronic structure. The conduction mechanism is based on the motion of charged defects within the conjugated framework, and strongly depends on the level of doping [32]. Typical examples are polyacetylene, polyaniline [33] and polyphenylenevinylene (PPV) [34]. Conducting polymers have been successfully utilized for commercial applications such as magnetic storage media, anti-static materials, electrolytic capacitors and batteries and much more. Extensive research efforts were devoted to optimization of the optical and electrical properties of conducting polymers, mainly via the development of efficient pathways for doping [32].

Recently it was demonstrated that MWNT could be used for doping of a conjugated luminescent polymer, poly(*m*-phenylenevinylene-*co*-2,3-dioctoxy-pphenylene-vinylene) (P*m*PV) [35] and polyaniline [36]. It was found that the electronic structure of P*m*PV [37] as well as other types of conducting polymers is modified by the presence of CNT [38] indicating strong coupling between the MWNT and the polymer π-systems. In a different system (ppyPV [38b]), it was found that SWNT promote the solution-protonation of the polymer, and consequentially affects its electrical properties. It is now well accepted that conjugated polymers and CNT are strongly associating, tightly bound systems. The molecular geometry of the association is that of (single or multi) helical wrapping of the tubes by the polymers [39]. The polymer-wrapped tubes form long-lived stable dispersions in different liquid media [40], and may be utilized for the preparation of CNT–polymer composites [41] exhibiting improved mechanical and electrical properties.

Strong binding and CNT–polymer-wrapping were also reported for a different type of coiling polymers, i.e. biopolymers such as DNA and peptides. Interactions between specific types of DNA and CNT enabled visualization of DNA [42] and affected the properties of CNT [43]. CNT–DNA complexes were found to form stable dispersions [44], enable fractionation of CNT [45] preparation of fibers and composites [46] as well as nano-electronic devices [47]. A comprehensive review of CNT–DNA interactions and related bio-applications is given in Ref. [48].

Recently Dieckmenn et al. [49] reported the synthesis and application of an amphiphilic peptide, specifically designed to disperse SWNT. It was observed that SWNT induce preferential folding of the peptide into specific configurations (α-helix), and the interactions among the SWNT-peptide moieties could be utilized for controlled self-assembly of the complexes. The concept is demonstrated in Fig. 7.

Dispersion of CNT via polymer wrapping was suggested in additional systems, where it was conjectured that wrapping leads to screening of the hydrophobic interaction at the CNT–water interface [50].
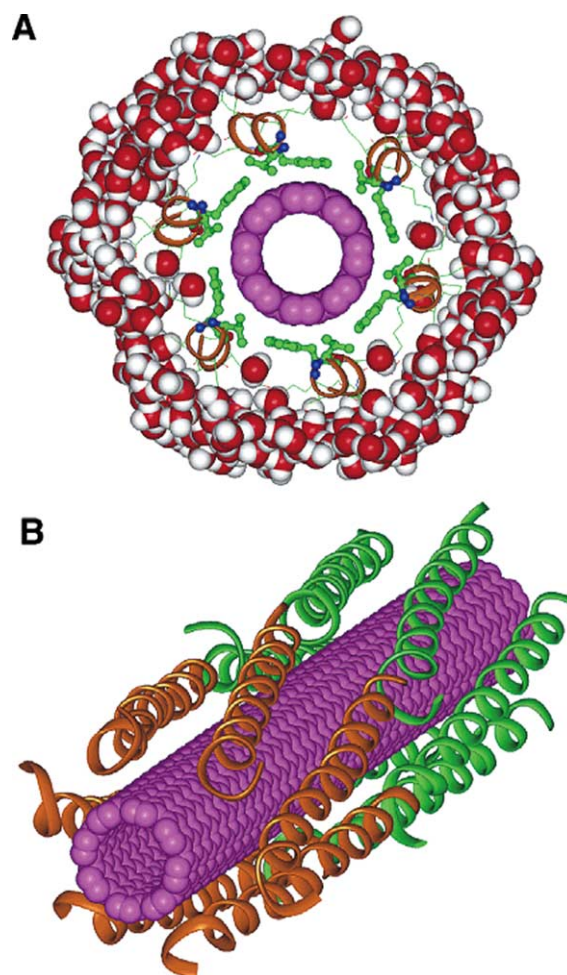

Fig. 7. A model illustrating the interaction between a synthetic, hydrophilic polypeptide, and an individual SWNT. (A) A cross section of an individual SWNT (pink) wrapped by six peptide helices, and a 5 Å thick water shell. (B) A side view of a peptide-wrapped SWNT (adapted with permission form Ref. [49]) (For interpretation of the references to color in this figure legend, the reader is referred to the web version of this article).

1.5. Polymers as entropic modifiers—shaping the phase behavior of CNT via weak non-specific interactions

A very different scenario is expected, and observed, in the absence of specific chemical interactions: the free energy of interaction between CNT decorated by adsorbed (or grafted) polymeric layers is then dominated by the polymers confined in the region between the two highly curved (cylindrical) surfaces. In these systems, polymer structure, surface forces, geometry and topology as well as dimensionality of the different components shape the range and depth of the intermolecular effective potential, and consequentially the phase behavior of the combined systems. As expected, entropic effects arising from the conformational degrees of freedom of the polymer molecules play the major role. In the following we discuss in detail each of the aspects that determine the effective CNT potentials in the presence of end attached polymers.

1.6. Nanotubes—a high(er) surface to volume ratio

A direct consequence (with non-trivial implications) of the nanometric diameter and almost macroscopic length of CNT is their relatively large surface area as compared to classical colloids. Thus, when CNT are embedded within a polymeric medium, the systems become enriched by interfacial zones that are subjected to non-bulk potentials and forces.

During the last 30 years there has been an immense amount of work describing the behavior of polymers at surfaces and interfaces [51]. Complete description of polymer–surface interactions is a multidimensional task in which the polymer and surface structure, molecular weight, polymer concentration and type of solvent combine to determine the end result. Here we present the generic aspects relevant to CNT.

Essentially, the presence of a surface reduces the conformational degrees of freedom of polymers due to excluded volume interactions [52]. This reduction in the number of allowed conformations, and thus in chains entropy, has two interrelated major consequences. First, the shape of polymers residing in close vicinity to the surface is altered with respect to that of polymers in the bulk. Second, the loss of entropy translates into a repulsive interaction between the polymers and the surface. Thus, in the absence of additional attractive interactions, polymers are depleted from surfaces. In colloidal dispersions this results in an effective attractive force between the colloidal particles, known as 'depletion force' [53]. The range of this force is of the order of the radius of gyration of the polymers. It is then possible to tune the range and strength of the effective attractions by modifying the polymer characteristic size and tailor the phase diagram of the combined systems. Indeed, it was demonstrated that the presence of polymers induces novel phase transitions in colloidal system [2b].

A different scenario arises in the presence of an attractive (enthalpic) interaction between the polymers and the surface. Attraction competes with the entropically driven repulsion, and leads to adsorption of polymeric chains. When the attractive component is localized (for example, at chain ends) the polymer molecules attach in a specific way to the surface, e.g. tether by their ends and may form a dense layer known as a 'polymer brush' [54]. This additional restriction on the polymeric molecules results in a more severe entropic penalty leading to an even more dramatic change in the range and strength of the interactions. This case will be discussed in more detail in the sections below.

The high surface-to-volume ratio in CNT-filled polymers is manifested in a variety of surface-related effects: an increased degree of crystallinity was observed in semicrystalline matrices, with a clear dependence on the volume fraction of CNT [55]. Enhancement of the crystallization rate [56] modification of the glass transition [57], and improvement of the mechanical properties were reported [58].

It was suggested that some of the synergetic effects in polymer–CNT systems may be used for preparation of new types of structural–functional materials. A few examples out of a very long and exciting list are mentioned below: CNT were used to trigger shape change in CNT-filled thermoplastic elastomers in response to external stimuli, enabling the use of the composites as active materials [59]. Stress transfer via the polymeric interlayer in CNT–polymer fibers [60] and improved thermal conductivity were demonstrated [61].

1.7. Geometry and topology-the aspect ratio

Another aspect of reduced dimensionality realized in non-spherical nano-objects, is an extreme aspect ratio. For example, micron long SWNT exhibit an aspect ratio of 1000 or more [7]. When combined with a high persistence length [11], a rich phase behavior emerges including different demonstrations of lyotropic liquid crystalline phases [11, 62].

When used as fillers in polymeric matrices the high aspect ratio of CNT results in the formation of a connected CNT-network at low volume fraction. The transition is known as the percolation threshold [63]. A marked increase in the mechanical strength and electrical conductivity are observed above percolation, as the connected network simultaneously provides a mechanical backbone and a pathway for electrical conductivity. Electrical percolation thresholds below 0.1 wt% of SWNT were reported in several polymeric matrices [64], suggesting that CNT–polymer nanocomposites may be utilized for antistatic shielding, shielding of electromagnetic interference, and preparation of transparent conductors [65].

An interesting observation is that though the reported percolation values are about two orders of magnitude lower than the value for carbon black (a colloidal filler), these values are many times higher than the theoretical predictions for randomly oriented objects of similar aspect ratio [66]. The measured values were often attributed to experimental flaws such as a low quality of the electrical contacts between polymer coated CNT. Yet, it was recently suggested [67] that the effect may be inherent and originate from intermolecular interactions. Both an analytical model and numerical simulations were used to demonstrate that intermolecular interactions that lead to partial alignment of the tubes within the matrix might significantly increase the expected bulk percolation threshold. This example demonstrates nicely the complexity of CNT–polymer systems, as it shows that the non-isotropic shape of the tubes, which results in orientation dependent interfacial interactions, affects the bulk conductivity in composite materials.

Another important issue is that of controlled or predictable self assembly of nano-objects. Indeed this is
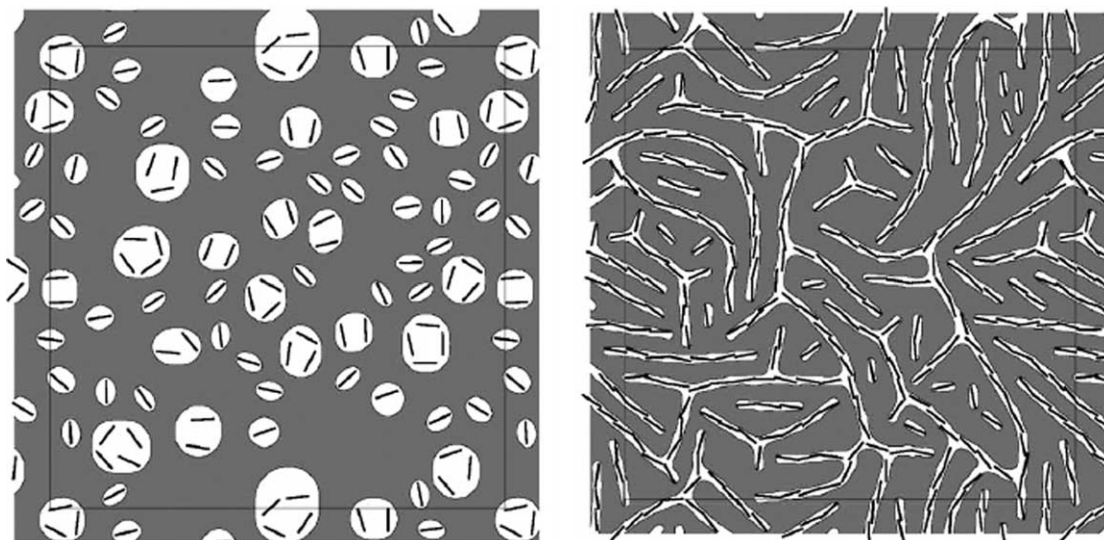
Fig. 8. Morphology of nanorod–polymer blend for (a) 2% and (b) 6% volume fraction of nanorods. White regions are the minority phase, gray regions are the majority phase (adapted with permission from Ref. [69]).

one of the more challenging goals on the route towards development of functional nano-composites. Recently it was suggested by Balazs et al. [68] that phase separation of non-fully miscible polymer blends may be utilized for driving self-assembly of nano-rods dispersed in one of the phases, into supramolecular three-dimensional networks. It is well known that most polymers are immiscible over most of the temperature range due to the insignificant gain in mixing entropy. Thus, polymer blends tend to phase separate, forming a rich collection of morphological structures. Phase morphology controls the impact strength, transparency, and conductivity of the resulting composites [69]. In the combined nano-rods–polymer system, the phase behavior of the blend components, surface interactions, and anisotropic inter-rod interactions determine the morphology of this complex system and in particular the formation of self-assembled structures of nanorods. Using different simulation techniques Buxton and Balazs [69] investigated the morphological evolution of the nanorodes–blend system as well as the mechanical and electrical properties of the resulting nano-composite. Their observations suggest that selective incorporation of nanorods into the minority phase of a phase-separating polymer blend affects the domain morphology of the polymers and drives selfassembly of the nanorods. The mutual interactions result in the emergence of a doubly percolating network of the polymer minority phase and the nano-rods, the latter at a volume fraction much lower than that observed in a homogeneous melt [69], Fig. 8.

1.8. Nanometric dimensions—what's in a scale

While the first two features described above demonstrate an enhancement and amplification of colloidal properties,

colloids and nanotubes differ by an inherent property: the inter-particle potential. Classical colloids are mesosocopic objects and dominated, in general, by long-ranged dispersive forces[1], while fullerens [70] and SWNT are large molecules and interact via a short-ranged intermolecular potentials [71]. The difference originates from the fact that SWNT and fullerenes are hollow structures with two (SWNT) or three (fullerenes) nanometric dimensions.

The resulting phase diagrams display condensed phases at a very narrow temperature range, as was thoroughly discussed in the context of fullerens [72].

Below we discuss in detail the effect of dimensionality on the interaction potential.

The intermolecular interaction potential between two individual SWNT in vacuum were derived using the Girifalco et al. model [71]. As presented in Fig. 9, a large attractive interaction at short inter-tube distance (less than 2 nm) is observed, with a minimum of about 40 kT/nm. The short ranged attraction decreases to below kT within 2.5 nm.

Consider two 1 μm long tubes at contact with each other, the potential shown in Fig. 9 predicts a contact energy of 40,000 times the thermal energy! Clearly, there will be a very large tendency of the tubes to be found in the form of bundles, as experimentally observed [5]. Indeed all the strategies developed for de-bundling CNT aim to modify the inter-tube potential. As conventional wisdom would suggest, reduction of the attractive minimum via chemical

---

[1] It should be mentioned that the attractive interactions between colloidal particles are proportional to the effective Hamaker constant. Therefore, by properly changing the medium, where the particles are dispersed it is possible to achieve short-range attractive interactions for large colloidal particles. However, the presence of large vdW attractions with a range of a few times the particles size is the most common case [90].
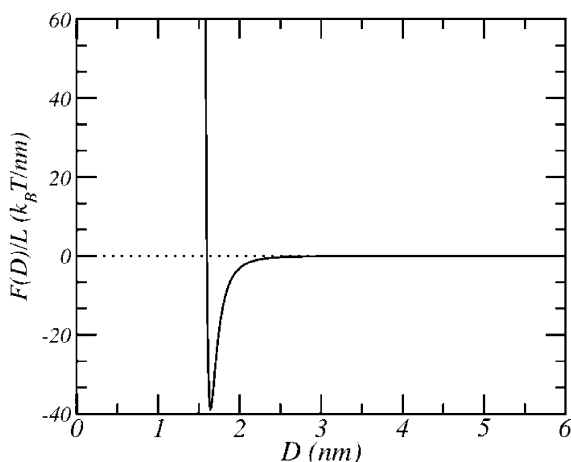
Fig. 9. The specific interaction potential between two parallel SWNT as a function of the distance between them, (following Ref. [71]).

modification of the extended π-systems (the origin of the strong vdW attraction), or the introduction of electrostatic repulsion, should enable exfoliation and dispersion of CNT. Yet (as described above), this approach leads to inherent diminishment of the unique properties of the individual tube. A different approach would be to take advantage of the short range of the potential: the behavior of objects interacting via a short ranged attraction is known to be highly sensitive to variations in the long-range tail of the inter-particle potential [2,72]. Thus, a relatively weak, but long ranged repulsion, such as the osmotic (steric) repulsion among tails of tethered copolymers, in good solvent conditions [73], may lead to significant modification of the CNT phase behavior. Weak, long-ranged interactions are not expected to interfere with the electronic structure of the tubes or modify the physical properties of the individual tube. A possible scenario leading to steric stabilization of individual SWNT in polymeric solutions is described below.

1.9. Utilizing entropic interactions for dispersing CNT in polymeric solutions

It was recently demonstrated that steric repulsion among polymer-decorated tubes can be employed for stabilization of CNT dispersions [74]. As the approach does not rely on specific interactions, it is efficient for both aqueous and organic media [75]. Among the more efficient steric stabilizers are block-copolymers and end functionalized polymers [2a]. Block copolymers are comprised of covalently bonded chemically distinct and often mutually incompatible moieties (designated A–B and A–B–A for di-blocks and tri-blocks, respectively) [76].

A model system which provides an upper bound for the repulsive interaction induced by attached polymers is a dense stretched 'polymer brush'. The strongest effect is expected when end-attached polymers assemble at a surface, in a good solvent environment and high surface coverage. The tethered chains stretch out in order to avoid intermolecular repulsions. In the so called 'brush regime' the thickness of the tethered polymer layer, h, scales with the polymer chain length, N, and polymer surface coverage, σ, as $h \propto N\sigma^{1/3}$ [54,77,78]. The linear increase of the thickness with molecular weight serves as an important tool in the manipulation of the range of the interactions. The interactions between planar tethered layers have been discussed at length elsewhere [78], however, we describe some of their properties here in order to show the dramatic effect of surface geometry on polymer packing and surface interactions.

An example of the effective steric repulsion induced by polymer layers tethered on planar surfaces is shown in Fig. 10. We apply a molecular theory that has been shown to provide quantitative predictions of the thermodynamic and structural properties of tethered polymer layers. A review of the theory, comparison with experimental observations and description of the model polymer used in the calculations can be found in Refs. [78b–80].

The two graphs present the steric interaction for two different polymer chain lengths. For each chain length, results for three different values of surface coverage are presented, from relatively low to high, all within the experimentally accessible range. Surface coverage highly affects both the range and the strength of the potential. Furthermore, we can see that longer chains increase the range of the interactions and the absolute strength of the repulsion for identical density of tethered chains. We find that the higher the surface coverage, the larger the distance at which the repulsive interaction diverges. This is due to overcrowding of polymer segments that occur as the distance between the surfaces decreases. To quantify this effect, Fig. 11 shows the volume fraction profiles for polymer chains corresponding to the intermediate surface coverage shown in Fig. 10 at two different distances between the surfaces: one corresponds to infinite distance, i.e. a single tethered polymer layer, and the other corresponds to the minimal distance shown for the interacting potential, i.e. the structure that corresponds to a repulsion of 90 kT/nm².

The volume fraction profiles show that upon reduction of the distance between the walls, polymer segments over-crowd in a narrow region of space. As the polymer segments cannot escape the confined region, an entropy loss prevails. This effect couples with displacement of solvent, resulting in a large osmotic price. The two effects are the origin of the repulsive interactions potentials shown in Fig. 10.

The typical diameter of CNT is significantly smaller than the radius of gyration of long polymer chains in good solvent conditions. We thus expect that chains tethered to tubes will exhibit different chain packing and tube-tube interactions than those exhibited by chains tethered to large colloidal particles. Clearly, as two nanotubes approach each other, the intertube region is different than the region between two planar surfaces.
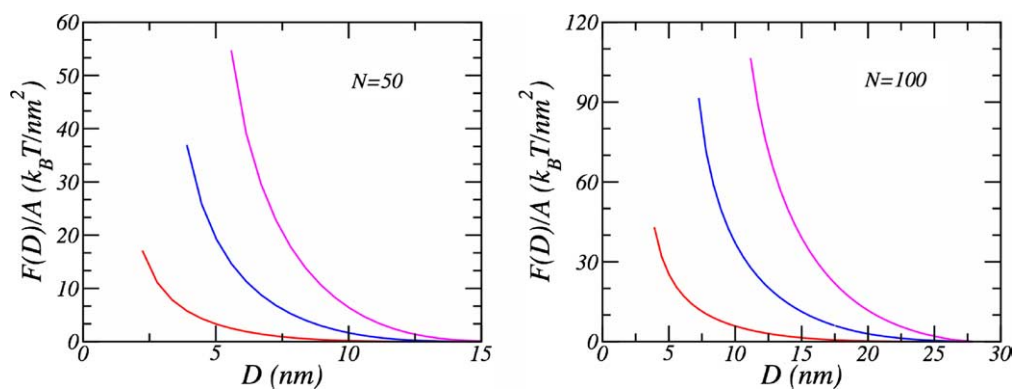
Fig. 10. Repulsive interactions between grafted polymers on planar surfaces, as a function of the distance between the grafting surfaces, as calculated from a molecular theory [78b]. The different colors represent different surface coverage: 0.032 nm^{-2} (red line); 0.064 nm^{-2} (blue line) and 0.096 nm^{-2} (magenta line) (For interpretation of the references to color in this figure legend, the reader is referred to the web version of this article).

Indeed, in the case of chains tethered to a CNT surface, with a typical diameter of the order of 1 nm, the chains can reduce the effect of confinement by re-arranging in space, at all angles surrounding the CNT. Fig. 12 shows the volume fraction of chains tethered on the surface of an isolated CNT. The density profile is presented as a function of the position in the plane perpendicular to the tubes. The figure shows a perfectly symmetric distribution of segments around the tube and though the density of attached polymers is high, the decay of the polymer volume fraction is much faster than the highly stretched profile shown in Fig. 11 (red curve). This is very similar to previously predicted behavior for polymers grafted to a line [81]. The volume available to the polymer chains as a function of the radial distance from the tube enables the chains to explore more of the conformational space than an equivalent chain tethered on a planar surface. Therefore, one would expect that the interaction potential between two CNT decorated with tethered polymers differ from that of planar surfaces.

Fig. 13 shows the steric repulsion between two polymer–decorated CNT for two different polymer molecular weights, as calculated using the molecular theory. In each case we show three different surface densities. In all cases,

as the distance between the parallel tubes decreases, the repulsion increases. The variation of the effective potential with distance is rather different from that of polymers grafted to planar surfaces: first, the derivative of the potential (the force) is much weaker at all tube–tube distances. Second, the distance of closest approach for two tubes is contact.

Third, polymers end-attached to CNT exhibit repulsions at a range shorter than that of polymers attached to planar surfaces. While the overall repulsion is weaker than that observed for polymers grafted to flat surfaces, short chains at low surface coverage show significant repulsions at an inter-tube distance of 3 nm. At this separation tubes attractions are already below the thermal energy, Fig. 9.

Before we present explicitly the overall interaction potentials, we discuss the origins of the relatively weak repulsive interactions. Fig. 14 shows the volume fraction profiles of two polymer-coated CNTs for two different separations. The large separation case is equivalent to two-isolated CNT. The second example shows the volume fraction profile at an inter-tube distance of the order of the tube diameter.
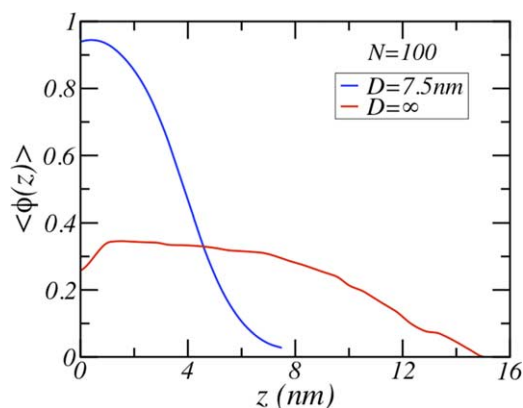

Fig. 11. Polymer volume fraction profile for chains originating on one planar surface for two different surface separations as marked on the legend $N=100$ and $\sigma=0.064$ nm^{-2}.
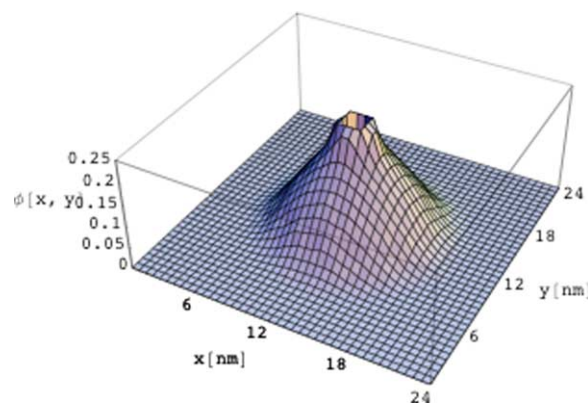

Fig. 12. The polymer volume fraction (in the plane perpendicular to the CNT) as a function of the distance (in nm) from the center of the tube. The chain length is $N=50$ and the line density 3.3 nm^{-1}. The hollow part in the center show the position of the tube.
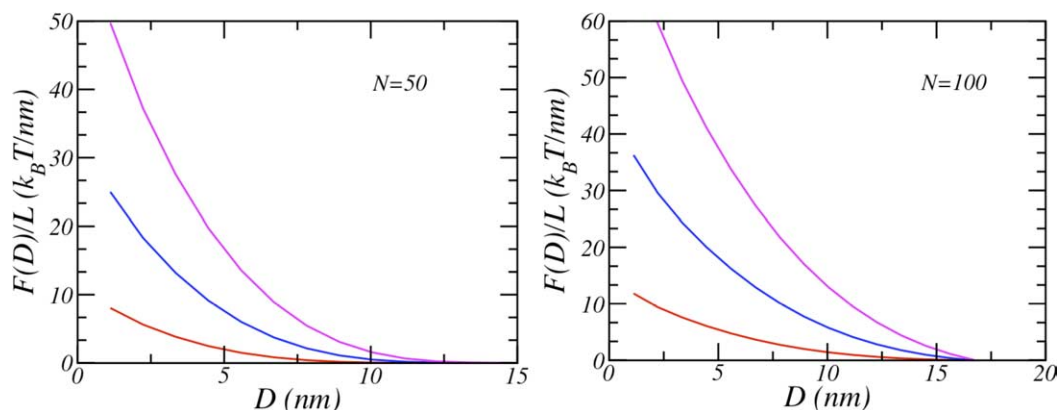
Fig. 13. The repulsive interactions between parallel CNT coated with endtethered polymers at different line densities, as a function of the distance between the CNT centers. The two graphs represent different polymer chain lengths as marked in the figures. The different colors represent different surface coverage: 2 nm^{-1} (red line); 3.3 nm^{-1} (blue line) and 4.7 nm^{-1} (magenta line) (For interpretation of the references to color in this figure legend, the reader is referred to the web version of this article).

Higher density of polymeric segments is found in the outer regions while the number of segments in the inter-tube region is reduced. In Fig. 15 we present the difference between the polymer volume fraction around an isolated CNT and the polymer volume fraction around the same tube but with a neighboring polymer-coated tube at 1.2 nm. The figure shows that there is a large depletion of polymer segments from the inter-tube region (negative values in the figure), towards the back of the tube, where the difference is positive, i.e. we observe an increased polymer concentration. Thus, the system can relax some of the strong repulsions by 'rotating' the chains towards less occupied regions. Note that, as shown in Fig. 11, polymers end-attached to planar or colloidal surfaces cannot relax in the same manner, resulting in a divergence of the repulsive interactions as shown in Fig. 10.

Are the repulsions triggered by end-adsorbed polymers (Fig. 13) strong enough to prevent the tubes from reaching the strongly attractive inter-tube region? To answer this question we present the combined profiles in Fig. 16. Note the presence of a repulsive barrier with a magnitude that depends upon the polymer surface coverage and chain

length. The maximum is found at an inter-tube distance of about 3–5 nm for all cases. Furthermore, a local minimum positioned at the same location as that of the bare CNT shown in Fig. 9, is observed in all the cases.

The shape of the potentials shown in Fig. 16 and the fact that even relatively short polymer chains suffice to create a high enough barrier and prevent tube aggregation, is a result of the (short) range of the CNT attraction. As described above, the latter is a direct consequence of the nanoscopic dimensions of CNT and the relative low density of interacting atoms due to the hollow nature of the tubes.

The results presented above, apply to stabilization of exfoliated CNT. Yet, a relevant and important question is what happens when polymer chains are tethered at the surface of CNT bundles? To answer this question we first determine the effective attractions between CNT bundles, using four-tube bundles to demonstrate the effect. Clearly, the driving force for bundle formation is the strong attractions between CNT shown in Fig. 9. We calculate the bundle–bundle interactions by adding the CNT–CNT inter-bundle interactions. The results are shown in Fig. 17. The attractive well is much deeper than for single CNT
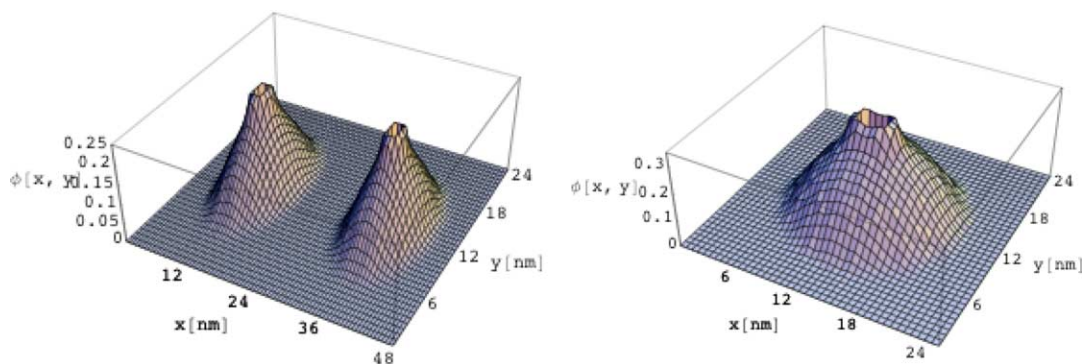

Fig. 14. The polymer volume fraction, in the plane perpendicular to the CNT, as a function of the distance (in nm) from the center of two parallel tubes. The left graph corresponds to a distance between the tubes of $D = 14$ nm, while the right graph corresponds to $D = 1.2$ nm. In both cases the polymer line density is 3.3 nm^{-1}.
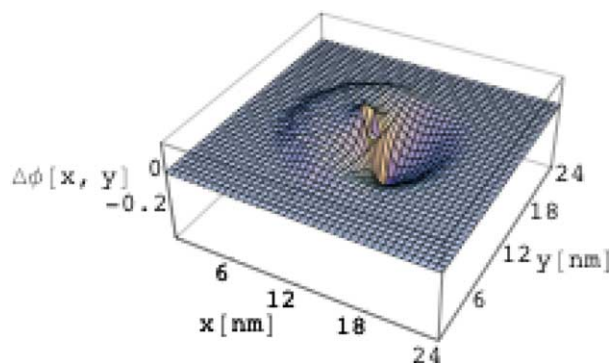
Fig. 15. The difference in polymer volume fraction between infinite distance and close contact, i.e. between the polymers coating the left nanotube in the two graphs shown in Fig. 14.

Fig. 17. The vdW interaction between two 4-tubes bundles. Also shown for comparison is the SCNT interaction from Fig. 9.

(SCNT) with a minimum of almost 90 times the thermal energy. The range of the interactions is also affected, as the location of the minimum is now found at an inter-bundle distance of about 2.75 nm and the attractions decay to values comparable to the thermal energy at an inter-bundles distance of 4 nm.

The strength and range of the inter-bundle potential suggest that while polymer-induced repulsion was effective in preventing aggregation of individual tubes, leading to dispersion of individual CNT in solution, it does not suffice in the case of small bundles. To this end Fig. 18 presents the total inter-bundle interactions of bundles decorated by end-attached polymer layers. We find that only long polymers form a barrier of about 20 kT/nm, while the barrier formed by the shorter molecular weight is less than half of that value. Note that a similar density of polymers resulted in a repulsive barrier of more than 40 kT/nm, in the case of individual tubes with $N=100$. We conclude that formation of stable dispersions of CNT bundles would require relatively long polymers at high grafting densities. Alternatively, the use of relatively short chain polymers for selective dispersion of individual CNT and small (<4 tubes) bundles offers a generic approach for preparation of dispersions of individual CNT.
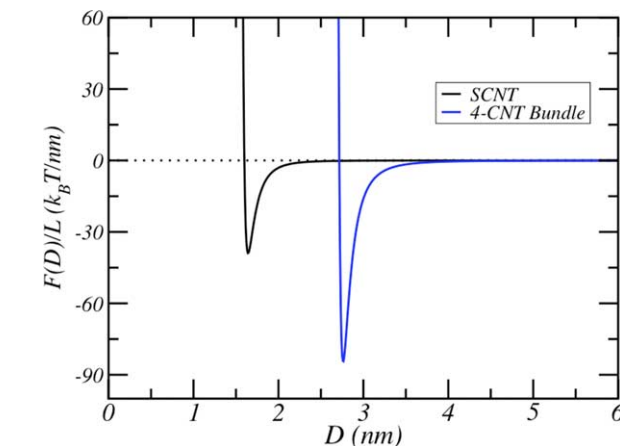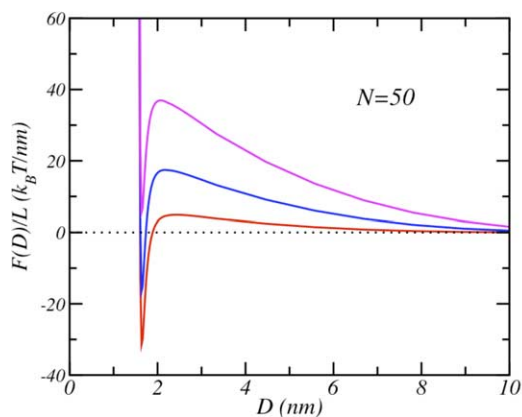
To summarize the theoretical studies, CNT exhibit strong, short ranged, attractive vdW interaction. The range of the interaction is determined by the nanometric length scale characteristic of two of the three dimensions of the tubes. Polymers attached at the surface of CNT introduce a repulsive (steric) barrier whose range and strength can be controlled by the polymer chain length and surface density. Increasing the polymer molecular weight results in a longer-range repulsive interaction. Moreover, increasing the density of (grafted, adsorbed) polymers increases the strength of the repulsive interactions.

It is important to emphasize that due to the geometry of the tubes the strength and range of the steric repulsion induced by the tethered polymer layers is qualitatively different than the steric repulsion between polymer chains grafted to planar surfaces.

It is well known, that the range of the attractive vdW interactions between particles is determined by the dimensions of the particle. In general the interaction range is a few times the particle size. Thus, in the case of CNT the range of the attractive interactions is a couple of nanometers and adsorption of relatively short polymers, in good solvent
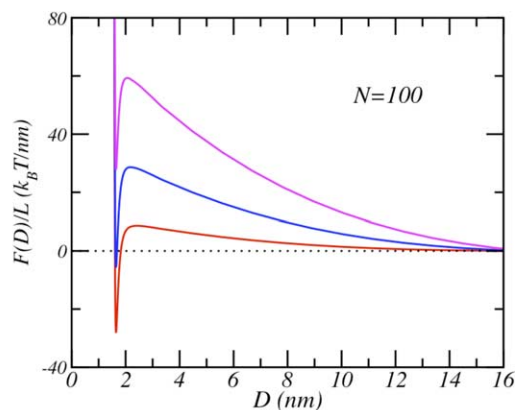

Fig. 16. The total interaction potential between parallel CNT. The potentials are obtained by adding the vdW attractive contribution, Fig. 9, and the steric repulsions arising from the tethered polymers, Fig. 13. The lines correspond to the same conditions as in Fig. 13.
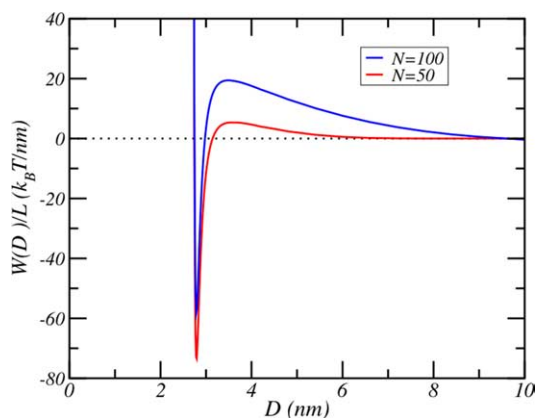
Fig. 18. The total interaction between polymer coated bundles composed by 4 CNT each. The polymer line density is $4 \, nm^{-1}$ and the polymer molecular weights are denoted in the figure.

conditions, suffices to present a steric barrier at a distance larger than the attractive inter-tube minimum, preventing tube aggregation. As for bundles, we showed that 4-tube bundles exhibit 7 times (approximately) deeper attraction at twice the range of that of the individual CNT. Thus, dispersion and prevention of bundle aggregation would require the tethering of much longer polymer chains at a higher density. These ideas were recently used by us for devising methods for selective dispersion of individual CNT from mixtures of bundles and colloidal particles.

1.10. From theoretical predictions to experimental results

The insight developed above may be utilized for development of generic, simple methods for dispersing individual CNT. As was demonstrated recently [74,75] a typical scenario may utilize mild sonication (which does not damage the tubes [82]) for exfoliation of the SWNT bundles, followed by adsorption or tethering of polymers. As long as the solvent acts as a good solvent for the attached polymer the dispersions are stable. A scheme summarizing this approach is presented in Fig. 19.

1.11. Practical recipes for dispersion of CNT—chemical considerations

The physical principles discussed above may be realized by utilizing block-copolymers and end-grafted macromolecules of specific chemical composition as dispersing agents, coupling agents and adhesion promoters [83,84] in polymeric matrices. The terms used above describe the action of a block-copolymers at the filler-melt interface: when the two blocks are chosen so that one of them is chemically compatible with the target matrix, while the other adsorbs at the filler surface, the polymer reduces the interfacial energy, leading to good adhesion at the individual tube–matrix interface, and thus improves

significantly the properties of SWNT-based composite materials [84].

Currently a large variety of off-the-shelf products is available. In addition, over the last 10 years new techniques have been developed and old techniques refined to enable the synthesis of specifically functionalized polymers and new types of block copolymers. Most block copolymers used today are prepared by anionic polymerization [84,85]. Chemical modification of a selected block enables the preparation of a variety of polymers (including functional groups such as styrene/diene, fluorinated moieties, methacrylates and more) with a vast range of properties. In addition, the recently developed procedure known as controlled radical polymerization (CRP), which utilizes living free radical polymerization enables the preparation of practically any kind of vinyl monomers-based polymers [85].

Thus, once a specific polymeric matrix is defined as a target material for preparation of CNT–polymer composite, a proper dispersing and compatibilizing agent may be tailored and synthesized. In the following we use two specific examples to demonstrate the concept.

The first example relates to polydimethylsiloxane (PDMS)–CNT composites. PDMS is one of the highly used elastomers, yet native PDMS is of low modulus and durability. Thus most applications rely on reinforcement by fillers. PDMS–CNT composites are expected to exhibit improved properties as compared to silica and carbon-black composites, due to the expected increase in the mechanical strength as well as electrical conductivity at low percolation thresholds. The resulting CNT-PDMS nanocomposites may be utilized for antistatic shielding, shielding of electromagnetic interference, and preparation of transparent conductors.

CNT–PDMS composite may be easily prepared using a tri-block copolymer poly(ethyleneoxide-b-polydimethylsiloxane-b-ethyleneoxide) (PEO–PDMS–PEO) as both the dispersing agent for CNT and the coupling agent to the matrix. A solution of PEO-PDMS-PEO is prepared in heptane, which is a poor solvent for the PEO moiety while being a good solvent for PDMS. Once CNT is sonicated in the solution (Fig. 19) the block copolymer adsorbs to the exfoliated CNT surface and induces steric repulsion among the dangling PDMS loops. The formation of a CNT–PDMS composite [86] is then straight forward: PDMS is co-dissolved in the CNT–block-copolymer dispersion followed by evaporation of the solvent that results in the formation of a macroscopically homogenous composite [86].

The second example relates to a very different, water soluble matrix, an acrylic ester copolymer (a commercial product is the Acronal series produced by BASF, Germany). Following the procedure described above, using Pluronic P123 tri-block copolymer—poly(ethyleneoxide)-b-poly(propyleneoxide)-b-poly(ethylene oxide) termed PEO_{20}–PPO_{70}–PEO_{20}, as the dispersing agent and water as the solvent, results in the formation of CNT–Acronal
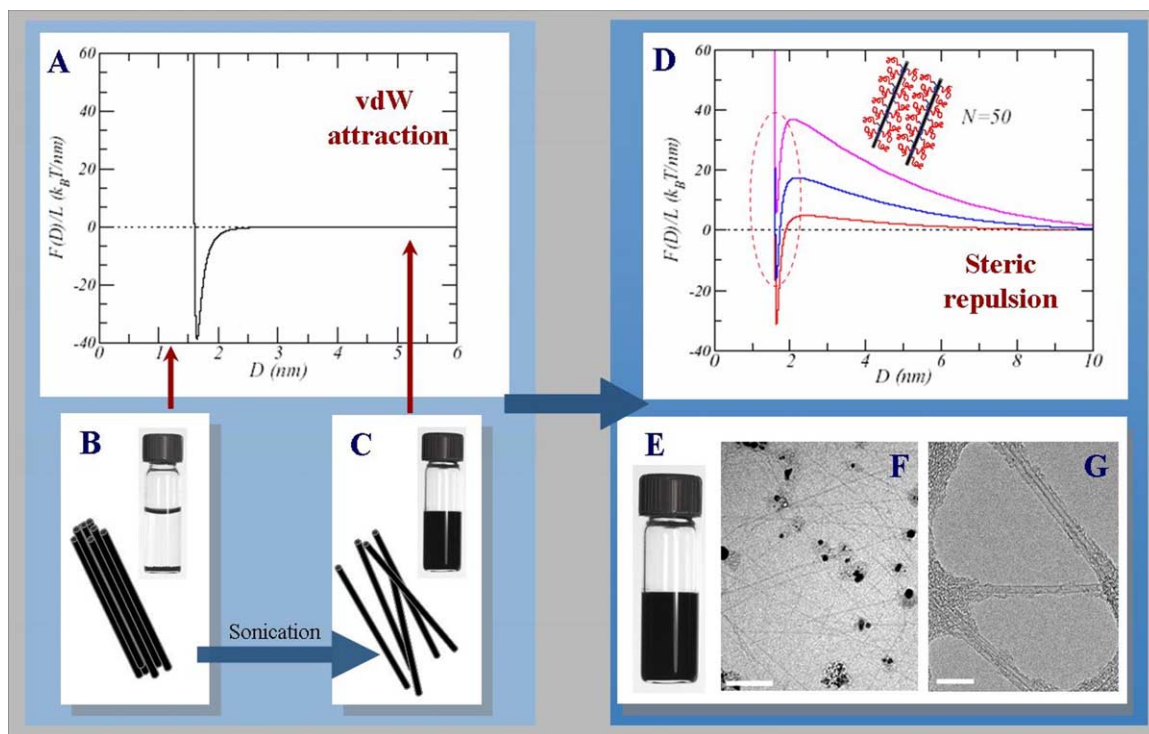
Fig. 19. A schematic representation of the concept. (A) Total interaction energy vs. the separation distance D, for two nanotubes. (B) The dry CNT powder is composed of bundled SWNT. (C) Sonication leads to temporary exfoliation of the powder followed by re-aggregation. (D) Formation of a polymer brush modifies the inter-tube potential due to steric repulsion. Macroscopic (E) and microscopic imaging of the black dispersions indicate that the dispersion is composed of individual tubes and small bundles (F) Cryo-TEM image (scale bar = 100 nm) and (G) HRTEM image (scale bar = 10 nm). Adapted from Ref. [74].

composites. We have recently demonstrated that in both cases the CNT filler is well dispersed within the matrix and forms low percolation threshold matrices [86].

By adopting a similar approach it is expected that CNT—polymeric composites could be prepared in different matrices using for melt and solution blending [87], electron spinning of CNT–polymer fibers [88] and new approaches of self-assembly [84,89,90], while preserving the unique properties of the un-modified tubes.

2. Conclusions

The field of CNT–polymer composites is currently undergoing rapid developments. Over the last few years it has been demonstrated that polymers can serve as efficient tools for engineering the interfacial behavior of CNT without damaging the unique properties of the individual tube. Polymers were shown to be efficient tools for dispersing, separating, assembling and organizing CNT in different media.

It is evident that harnessing the unique physical properties CNT in materials applications would require the development of a thorough understanding of the complex polymer–CNT system. While a variety of observations concerning polymer–CNT systems may be understood using well studied concepts from polymer physics and colloid science, other observations suggest the existence of unique phenomena that may rationalized via new concepts related to the unique electronic structure and dimensionality of CNT.

References

[1] (a) Encyclopedia Britannica, Chicago, IL: William Benton; 1966, p. 257–259.
(b) de Gennes PG, Badoz J. Fragile objects: soft matter, hard science, and the thrill of discovery. Berlin: Springer; 1996, p. 29.
[2] (a) Napper DH, editor. Polymeric stabilization of colloidal dispersions. Orlando, FL: Academic Press; 1993.

(b) For a recent review of a theoretical approach to polymer and colloids, see Fuchs M, Schweizer KS. J Phys: Condens Matter 2002;14:R239–R69 [and references therein].

[3] (a) Ajayan PM, Ebbesen TW. Rep Prog Phys 1997;60:1026.

(b) Dresselhaus MS, Dresselhaus G, Eklund PC. Science of fullerenes and carbon nanotubes: their properties and applications. Orlando, FL: Academic Press; 1996.

[4] Iijima S. Nature 1991;354:56–8.

[5] (a) Ijima S, Ichihasui T. Nature 1993;363:603.

(b) Thess A, Lee R, Nikolaev P, Hongjie D, Petit P, Robert J, et al. Science 1996;273:483.

(c) Journet C, Maser WK, Bernier P, Loiseau A, Lamydela M, Chapelle M, et al. Nature 1997;388:756.

(d) Rinzler AG, Liu J, Dai H, Nikolaev P, Huffman CB, Rodriguesz-Macias F, et al. Appl Phys 1998;A67:29.

[6] Dresselhaus MS, Dresselhaus G, Avouris Ph. Carbon nanotubes, topics in applied physics. vol. 80. Berlin: Springer; 2001.

[7] (a) long SWNT are now easily prepared: Zhu HW, Xu CL, Wu DH, Wei BG, Vajtai R, Ajayan PM. Science 2002;296:886 [and 4 cm long SWNT].

(b) Zheng LX, O'Connell MJ, Doorn SK, Liao XZ, Zhao YH, Akhadov EA. Nat Mater 2004;3:673.

[8] www.seas.upenn.edu/mse/research/nanotubes.html

[9] Collins PG, Avouris P. Sci Am 2000;62.

[10] For comparison, the current density of copper is 10^6 A/cm^2.

[11] Frank SP, Poncharal P, Wang ZL, de Heer WA. Science 1998;280:1744.

[12] (a) Davis VA, Ericson LM, Nicholas A, Parra-Vasquez G, Fan H, Wang Y, et al. Macromolecules 2004;37:154.

(b) Salvetat JP, Kulik AJ, Bonard JM, Andrew G, Briggs D, Stockli T, et al. Adv Mater 1999;11:161.

[13] Yu MF, Files BS, Arepalli S, Ruoff RS. Phys Rev Lett 2000;84:5552.

[14] Tans SJ, Verschueren ARM, Dekker C. Nature 1998;393:49.

[15] Rinzler AG, Hafner JH, Nikolaev P, Lou L, Smalley E. Science 1995;269:1550.

[16] (a) de Heer WA, Chatelin A, Ugrate D. Science 1995;270:1179.

(b) Semet V, Binh VT, Vincent P, Guillot D, Teo KBK, Chhowalla M, et al. Appl Phys Lett 2002;81:343.

[17] Diehl MR, Yaliraki SN, Beckman RA, Barahona M, Heath JR. Angew Chem Int Ed 2002;41:354.

[18] (a) Tománek D, Enbody R, editors. Science and application of nanotubes. Dordrecht: Kluwer Academic Publishers; 2000.

(b) Smith JG, Connell JW, Delozier DM, Lillehei PT, Watson KA, Lin Y, et al. Polymer 2004;45:825.

[19] (a) Ajayan PM, Charlier JC, Rinzler AG. Proc Natl Acad Sci 1996;96:14199.

(b) Baughman RH, Zakhidov AA, de Heer WA. Science 2002;297:792 [and references therein].

(c) See also NASA, Johnson Space Center: the nanomaterials project (http://mmptdpublic.jsc.nasa.gov/jscnano/).

[20] Niu C, Sichel EK, Hoch R, Moy D, Tennent H. Appl Phys Lett 1997;70:1480.

[21] Kong J, Franklin NR, Zhou C, Capline MG, Peng S, Cho K, et al. Science 2000;287:622.

[22] (a) Mattson MP, Haddon RC, Rao AM. J Mol Neurosci 2000;14:175.

(b) Chen X, Lee GS, Zettle A, Betozzi CR. Angew Chem Int Ed 2004;43:6111.

[23] As-prepared arc-discharge SWNT, adapted from Cohen, R; Master thesis, BGU 2005. The SWNT sample was purchased from Nano carblab (NCL) Russia. The images were taken by Dr Yeal Levi Kalisman, the ILSE KATZ Center for Meso and Nanoscale Science and Technology, BGU, Beer Sheva.

[24] The different samples are: (a) SWNT select grade (purity of 85 vol%) and (b) SWNT AP grade (purity of 50–70 vol%), purchased form Carbolex, USA (www.carbolex.com) (c) SWNT (purity of 80 wt%) purchased form Nano Carblab (NCL), Russia (www.nanocarblab.com), (d) SWNT (purity of 50–70 wt%) were synthesized at the

Physical Chemistry Department, The University of Karlsruhe, Germany (see for example Lebedkin, Schweiss P, Renker B, et al. Carbon, 2002; 40: 417–423). The images were taken by Dr Yael Kalisman, The Ilze Katz Center for Meso and Nanoscale Science and Technology, Ben-Gurion University, Beer-Sheva, Israel.

[25] Derycke V, Martel R, Appenzeller J, Avouris Ph. Nano Lett 2001;1:456.

[26] Choi WB, Bae E, Kang D, Chae S, Cheong B-h, Ko J-h, et al. Nanotechnology 2004;S512–S6.

[27] Ajayan PM, Schadler LS, Giannaris C, Rubio A. Adv Mater 2000;12:750–3.

[28] (a) Chen J, Hamon MA, Hu H, Chen Y, Rao AM, Eklund PC, et al. Science 1998;282:98.

(b) Chen J, Rao A, Lyuksyutov S, Itkis ME, Hamon MA, Hu H, et al. Phys Chem B 2001;105:2525.

(c) Niyogi S, Hu H, Bhowmik P, Zhao B, Rozenzhak SM, Chen J, et al. J Am Chem Soc 2001;123:733.

(d) Zhao B, Hu H, Niyogi S, Itkis ME, Hamon MA, Bhowmik P, et al. J Am Chem Soc 2001;123:11673.

(e) Sun YP, Huang W, Lin Y, Fu K, Kitygorodskiy A, Riddle LA, et al. Chem Mater 2001;13:2864.

(f) Fu K, Huang W, Lin Y, Riddle LA, Carroll DL, Sun YP, et al. Nano Lett 2001;1:439.

(g) Nguyen CV, Delzeit L, Cassell AM, Li J, Han J, Myyapen M. Nano Lett 2002;2:1079.

(h) Shim M, Wong N, Kam S, Chen RJ, Li Y, Dai H, et al. Nano Lett 2002;4:285.

(i) Peng H, Alemany LB, Khabashesku VN, Margrave JL. J Am Chem Soc 2003;125:15174.

(j) Zhu J, Kim JD, Peng H, Margrave JL, Khabashesku V, Barrera EV. Nano Lett 2003;3:1107.

(k) Saini RK, Chiang IW, Peng H, Smalley RE, Billups WE, Hauge RH, et al. J Am Chem Soc 2003;125:3617.

(l) Hu H, Zhao B, Hamon MA, Kamaras K, Itkis ME, Haddon RC. J Am Chem Soc 2003;125:14893.

(m) Baek JB, Lyons CB, Tan LS. J Mater Chem 2004;14:2052.

[29] (a) Nakashima N, Tomonari Y, Murakami H. Chem Lett 2002;31:638.

(b) Zhm W, Minami N, Kazaoui S, Kim J. J Mater Chem 2004;1924.

[30] (a) Vigolo B, Penicaud A, Coulon C, Sauder C, Pailler R, Journet C, et al. Science 2000;290:1331.

(b) O'Connell MJ, Bachilo SM, Huffman CB, Moore VC, Strano MS, Haroz EH, et al. Science 2002;297:593.

(c) O'Connel MJ, Bachilo SM, Huffman CB, Moore VC, Strano MS, Haroz EH, et al. Science 2002;297:593.

(d) Richard C, Balavoine F, Schultz P, Ebbesen TW, Mioskowski C. Science 2003;300:775.

(e) Moore VC, Strano MS, Haroz EH, Hauge RH, Smalley RE, Schmidt J, et al. Nano Lett 2003;3:1379.

(f) Islam MF, Rojs DM, Johnson AT, Yodh AG. Nano Lett 2003;3:269.

(g) Regev O, El Kati PNB, Loos J, Koning CE. Adv Mater 2004;16:248.

(h) Kono J, Ostojic GN, Zaric S, Strano MS, Moore VC, Shaver J, et al. Appl Phys A 2004;78:1093.

(i) Wang H, Zhou W, Ho DL, Winey KI, Fischer JE, Glinka CJ, et al. Nano Lett 2004;9:1789.

[31] (a) Monthioux M, Smith BW, Claye A, Fischer JE, Luzzi DE. Carbon 2001;39:1251.

(b) Garg A, Sinnott SB. Chem Phys Lett 1998;295:273.

(c) Czerw R, Guo Z, Ajayan PM, Sun Y-P, Carroll DL. Nano Lett 2001;8:423–7.

(d) Chen J, Liu H, Weimer WA, Halls MD, Waldeck DH, Walker GC. Am Chem Soc 2002;124:9034.

[32] (a) Brédas JL, Silbey R. Conjugated polymers. Dordrecht: Kluwer Academic Publishers; 1991.
(b) Dai H, Mau AWH. J Phys Chem B 2000;104:1891.

[33] (a) Shirakawa H, Louis EJ, MacDiarmid AG, Chiang CK, Heeger AJ. J Chem Soc, Chem Commun 1977;578.
(b) Stejsnal J, Gilbert RG. Pure Appl Chem 2002;745:857.

[34] PPV Burroughes JH, Bradley DDC, Brown AR, Marks RN, Mackay K, Friend RH, et al. Nature 1990;347:539.

[35] (a) Curran SA, Ajayan PM, Blau WJ, Carroll DL, Coleman JN, Dalton AB, et al. Adv Mater 1998;14:1091.
(b) Curran S, Davey AP, Coleman JN, Dalton AB, McCarthy B, Maier S, et al. Synth Met 1999;103:2559.
(c) Coleman N, Dalton AB, Curran S, Rubio A, Davey AP, Drury A, et al. Adv Mater 2000;12:213.

[36] (a) Zengin H, Zhou W, Jin J, Czerw R, Smith DW, Echegoyen Jr L, et al. Adv Mater 2002;14:1480.
(b) Wu T-M, Lin Y-W, Liao C-S. Carbon 2005;43:734 [and references therein].

[37] Dalton AB, Blau WJ, Chambers G, Coleman JN, Henderson K, Lefrant S, et al. Synth Met 2001;121:1217.

[38] (a) Star A, Stoddart F, Steuerman D, Diehl M, Boukai A, Wong EW, et al. Angew Chem Int Ed 2001;409:1721.
(b) Steuerman DW, Star A, Narizzano R, Choi H, Ries RS, Nicolini C, et al. J Phys Chem B 2002;106:3124.

[39] Steuerman DW, Star A, Narizzano R, Choi H, Ries RS, Nicolini C, et al. J Phys Chem B 2002;106:3124.

[40] Rouse JH. Langmuir 2005;21:1055–61.

[41] (a) Star A, Liu Y, Grant K, Ridvan L, Stoddart JF, Steuerman DW, et al. Macromolecules 2003;36:553.
(b) Wang J, Dai J, Yarlagadda T. Langmuir 2005;21:9.

[42] Guo Z, Sadler PJ, Tsang SC. Adv Mater 1998;10:701.

[43] Chou SG, Ribeiro HB, Barros EB, Santos AP, Neizch D, Samsonidze GeG, et al. Chem Phys Lett 2004;397:296–301.

[44] Zheng M, Jagota A, Semke ED, Diner BA, Mclean RS, Lustig SR, et al. Nat Mater 2003;2:338.

[45] (a) Zheng M, Jagota A, Strano MS, Santos AP, Barone P, Chou SG, et al. Science 2003;302:1545.
(b) Guo Z, Sadler PJ, Tsang SC. Adv Mater 1998;10:701.

[46] (a) Matyshevska OP, Kavlash AY, Shtogun YV, Benilov A, Kiryizov Y, Gorchinskyy KO, et al. Mater Sci Eng 2001;C15:249.
(b) Erlanger BF, Chen BX, Zhu M, Brus L. Nano Lett 2001;1:465.
(c) Barisci JN, Tahhan M, Wallace GG, Badaire S, Vaugien T, Maugey M, et al. Adv Funct Mater 2004;14:133.

[47] Keren K, Berman SR, Buchstab E, Sivan U, Braun E. Science 2003; 302:1380–2.

[48] Gao H, King Y. Ann Rev Mater Res 2004;34:13–50.

[49] Dieckmann GR, Dalton AB, Johnson PA, Razal J, Chen J, Giordano GM, et al. J Am Chem Soc 2003;124:1770.

[50] (a) O'Connell MJ, Boul P, Ericson LM, Huffman C, Wang Y, Haroz E, et al. Chem Phys Lett 2001;342:265.
(b) Star A, Steuerman DW, Heath JR, Stoddart F. Angew Chem Int Ed 2002;41:2508.

[51] See for example Jones RAL, Richards RW. Polymers at surfaces and interfaces. Cambridge: Cambridge University Press; 1999.

[52] de Gennes PG. Scaling concepts in polymer physics. Ithaca, NY: Cornell University; 1979.

[53] (a) Joanny JF, Leibler L, de Gennes PG. J Polym Sci, Polym Phys Ed 1979;17:1073.
(b) de Gennes PG. Macromolecules 1980;13:1069–75.
(c) Binder K, Milchev A, Baschnagel J. Ann Rev Mater Sci 1996;26:107.
(d) Wu DT, Fredrickson GH, Carton JP, Ajdari A, Leibler L. J Polym Sci Part B: Polym Phys 1995;33:2372.

[54] Alexander S. J Phys (Paris) 1977;38:977.

[55] (a) Grady BP, Pompeo F, Shambaugh RL, Reaco DE. J Phys Chem B 2002;106:5852.
(b) Bin Y, Tanaka M. Macromolecules 2003;36:6213.

[55] (c) Czerw R, Guo Z, Ajayan PM, Sun Y-P, Carroll DL. Nano Lett 2001;1:423.
(d) A different scenario is described in Barber AH, Cohen SR, Wagner HD. Nano Lett 2004;4(8):1439–43.

[56] (a) Valentini L, Biagiotti J, Kenny JM, Santucci S. J Appl Polym Sci 2002;87:708–13.
(b) Bhattacharyya AR, Sreekumar TV, Liu T, Kumar S, Ericson LM, Hauge RH, et al. Polymer 2003;44:2373.

[57] (a) Wei C, Srivastava D, Cho K. Nano Lett 2002;2:647–50.
(b) Sreekumar TV, Liu T, Min BG, Guo H, Kumar S, Hauge RH, et al. Adv Mater 2004;16:58–61.

[58] (a) Dalton AB, Collins S, Razal J, Munoz E, Ebron VH, Kim BG, et al. J Mater Chem 2004;14:1.
(b) Cadek M, Coleman JN, Ryan KP, Nicolosi V, Bister G, Fonseca A, et al. Nano Lett 2004;4:353–6.

[59] Baughman RH, Cui C, Zakhidov AA, Iqbal Z, Barisci JN, Spinks GM, et al. Science 1999;284:1340.

[60] Qian D, Wagner GL, Liu WK, Yu M-F, Ruoff RS. Appl Mech Rev 2002;55:495.

[61] Biercuk MJ, Llaguno MC, Radosavljevic M, Hyun JK, Johnson AT, Fischer JE. Appl Phys Lett 2002;80:2767–9.

[62] (a) Kumar S, Dang TD, Arnold FE, Bhattacharyya AR, Min BG, Zhang X, et al. Macromolecules 2002;35:9039–43.
(b) Song W, Kinloch IA, Windle AH. Science 2003;302:1363.

[63] Stauffer D. Introduction to percolation theory. 1st ed. London: Taylor and Francis; 1985.

[64] (a) Grunlan JC, Mehrabi AR, Bannon MV, Bahr JL. Adv Mater 2004; 16:150.
(b) Kim B, Lee J, Yu I. J Appl Phys 2003;94:6724.
(c) Ramasubramaniam R, Chen J, Liu H. Appl Phys Lett 2003;83: 2928.

[65] Wu Z, Chen Z, Du X, Logan JM, Sippel J, Nikolou M, et al. Science 2004;305:1273.

[66] Balberg I, Binenbaum N, Wagner N. Phys Rev Lett 1984;52:1465.

[67] Grujicic M, Cao G, Roy WN. J Mater Sci 2004;39:4441.

[68] Peng G, Qiu F, Ginzburg VV, Jasnow D, Balazs AC. Science 2000; 288:1802.

[69] Buxton GA, Balazs AC. Mol Simul 2004;30:249.

[70] Girifalco LA. J Phys Chem 1992;96:858.

[71] Girifalco LA, Hodak M, Lee RS. Phys Rev B 2000;62:13104.

[72] (a) Costa D, Caccamo C, Abramo MC. J Phys: Condens Matter 2002; 14:2181.
(b) Schwarz US, Safran SA. Phys Rev E Part B 2000;62:6957.

[73] The quality of the solvent is characterized by the balance of inter vs. intra molecular interactions. In the mean field framework the Flory interaction parameter $\chi = \chi_{MS} - 1/2(\chi_{MM} + \chi_{SS})$ is used to describe the balance (where _mm is the monomer interaction, is the monomer solvent interaction and _ss is the solvent–solvent interaction). Good solvents are those characterized by low _, while poor (bad) solvents have a high _. A detailed description of the approach and a list of good and poor solvents for different polymers can be found in the handbook by Van Krevelen D.W. Properties of polymers. 3rd ed. Amsterdam: Elesvier; 1990.

[74] (a) Bandyopadhyaya R, Nativ-Roth E, Regev O, Yerushalmi-Rozen R. Nano Lett 2002;2:25.
(b) Shvartzman-Cohen R, Nativ-Roth E, Baskaran E, Levi-Kalisman Y, Szleifer I, Yerushalmi-Rozen R. J Am Chem Soc 2004;126:14850–7.

[75] Shvartzman-Cohen R, Levi-Kalisman Y, Nativ-Roth E, Yerushalmi-Rozen R. Langmuir 2004;20:6085.

[76] Hadjichristidis N, Pispas S, Floudas G. Block copolymers: synthetic strategies, physical properties, and applications. New York: Wiley; 2003.

[77] Halperin A, Tirell M, Lodge TP. Adv Polym Sci 1992;100:311.

[78] (a) Milner ST. Science 1996;905:251.
(b) Szleifer I, Carignano MA. Adv Chem Phys 1996;96:165.

[79] Szleifer I, Carignano MA. Macromol Rapid Commun 2000;21:423.

[80] (a) Carignano MA, Szleifer I. J Chem Phys 1994;100:3210.
     (b) Szleifer I. Curr Opin Colloid Interface Sci 1996;1:416.
[81] (a) Li H, Witten TA. Macromolecules 1994;27:449.
     (b) Murat M, Grest GS. Macromolecules 1991;24:704.
     (c) Carignano MA, Szleifer I. J Chem Phys 1995;102:8662.
[82] Strano MS, Moore VC, Miller MK, Allen MJ, Haroz EH, Kittrell C,
     et al. J Nanosci Nanotechnol 2003;3:81.
[83] Strano MS, Moore VC, Miller MK, Allen MJ, Haroz EH, Kittrell C,
     et al. J Nanosci Nanotechnol 2003;3:81.
[84] See for example Brown HR. Mater Forum 2000;24:49–58[http://
     www.mateng.asn.au/].
[85] Ruzette AV, Leibler L. Nat Mater 2005;4:19–31.
[86] Granick S, Kumar SK, Amis EJ, Antonietti M, Balazs AC,
     Chakraborty AK, et al. J Polym Sci Part B: Polym Phys 2003;41:
     2792.
[87] Bounioux C, Jopp J, Yerushalmi-Rozen R. In preparation.
[88] Grunlan JC, Mehrabi AR, Bannon MV, Bahr JL. Adv Mater 2004;16:150.
[89] Dror Y, Salalha W, Khalfin RL, Cohen Y, Yarin AL, Zussman E.
     Langmuir 2003;19:7102.
[90] Jung DH, Ko YK, Jung HT. Mater Sci Eng 2004;C24:117.

Rachel Yerushalmi-Rozen received her Ph.D. from the Weizmann Institute of Science in 1994. After a postdoctorate at the University of Minnesota she joined the department of Chemical Engineering at the Ben-Gurion University of the Negev. She is a member of the *Ilse Katz* Center for Meso- and Nanoscale Science and Technology. Her research interests are focused on experimental investigation of the behavior and properties of matter at the meso and nano scale with special emphasis on interfacial phenomena. Among the recent projects are studies of wetting and dewetting of simple and polymeric liquids, adsorption of polymers in confined geometries, entropic effects in polymer crystallization, formation of mesoporous materials the behavior of carbon nanotubes in polymer solutions and composites.

Igal Szleifer received his Ph.D. from the Hebrew University of Jerusalem, after a postdoctoral tenure at Cornell University; he joined the faculty at Purdue in 1991 where he is a Professor of Chemistry and the current Head of the Physical Chemistry Division. His research interest include the development and application of statistical mechanics to complex fluids, phase behavior and interfacial properties of polymers, polymer dynamics, with particular emphasis on polymer systems in confined environments and grafted polymers; interactions between proteins and polymer modified surfaces, thermodynamics and kinetics of proteins adsorption and liposome structure and behavior for drug delivery.